

I. UYGUR*

NOTCH BEHAVIOR AND FATIGUE LIFE PREDICTIONS OF DISCONTINUOUSLY REINFORCED MMCs

TEST UDARNOŚCI I PRZEWIDYWANIE WYTRZYMAŁOŚCI ZMĘCZENIOWEJ NIECIĄGLE UMACNIANYCH KOMPOZYTÓW METALOWO-CERAMICZNYCH

In this study, three notch geometries were assessed with different stress concentration factors. The severity of a notch increased with the stress concentration, hence the fatigue lives dramatically reduced due to increasing stress concentration factor. Fatigue life predictions for the notch geometries have been performed by using a critical strain life approach. It is shown that the model provides a reasonable fatigue life estimation for various notch geometries, volume fraction, and reinforcement particle size of the Al metal matrix composites. Typical crack initiation sites related with the particle clusters, large particles, and intermetallic particles. Although, crack propagation in the reinforced alloy occurred predominantly in the matrix material, SiC particles (SiC_p) played a significant role in influencing the crack path.

Keywords: MMCs, Fatigue, life prediction, notch behavior

W pracy, badano trzy geometrie karbu w powiązaniu z różnymi współczynnikami koncentracji naprężeń. Wielkość pęknięcia rosła z koncentracją naprężeń, a tym samym wytrzymałość zmęczeniowa była drastycznie obniżona ze względu na zwiększony współczynnik koncentracji naprężeń. Przewidywania trwałości zmęczeniowej dla różnych geometrii karbu zostały wykonane przy użyciu krytycznego czasu odkształcenia. Pokazano, że model umożliwia wystarczające szacowanie trwałości zmęczeniowej dla różnych geometrii karbu, frakcja objętości, i wielkości cząstek zbrojenia aluminiowych kompozytów metalowo-ceramicznych. Typowe miejsca inicjacji pęknięcia związane były z klastrami cząstek, dużymi cząstkami, i cząstkami intermetalików. Pomimo, że pęknięcia w kompozycie miały miejsce głównie w materiale matrycy, cząsteczki (SiC_p) odegrały znaczną rolę w kształtowaniu ścieżki pęknięcia.

1. Introduction

Discontinuously reinforced metal matrix composites (MMCs) are excellent candidates for structural components in the aerospace and automotive industries, where they are usually subjected to cyclic loads. The fatigue behavior of these composites has been received quite reasonable attention. The tensile responses [1], High Cycle Fatigue (HCF) responses [2], and Low Cycle Fatigue responses (LCF) [3] of Al-SiC_p composites were extensively investigated. An extensive review about the fatigue of materials and structures can be found in detail by Schijve [4]. The fatigue response of these MMCs has been influenced by the following properties: reinforcement type (continuous, whisker or particulate), volume fraction of reinforcement, composition, heat treatment, notch behavior, elevated temperatures, environment, and processing technique (casting or powder metallurgy) [5].

Fatigue analysis has become an early simulation in the product development process of a growing number of industries. In general, LCF involves large cycles with high amounts of plastic deformation and relatively short life. However, HCF is associated with low stresses and long life in which stresses and strains are largely confined to the elastic region. Fatigue analysis refers to three methodologies: i) local strain or crack initiation, ii) stresses life, and iii) crack growth or damage tolerance analysis. Most of fatigue life estimations depend on the methodology data mentioned above. However, many energy-based predictions have also been proposed in the literature [6]. It is almost impossible to avoid notches for most of engineering components. Due to stress concentrations (notches or defects), the local material yields firstly to redistribute the loading to the surrounding material, following with cyclic plastic deformation and mean stress relaxation. Predicting fatigue life is a critical

* DUZCE UNIVERSITY, FACULTY OF ENGINEERING, DEPARTMENT OF MECHANICAL ENGINEERING, KONURLAP CAMPUS, 81620, DUZCE-TURKEY

aspect of the design cycle because virtually every manufactured product will wear out or break down. In this study, fatigue data were applied to the early fatigue life methods based on the critical strain life approach, generating stress-life (S-N) and strain life (ϵ -N) curves to set safe operating conditions for service. The critical strain technique assumes that if a plain specimen and a notch are loaded under identical strain conditions, then they will fail in the same number of cycles. Hence, three different notch geometries with different stress concentration factors were used for the prediction of fatigue life.

2. Experimental procedures

Commercially 2124 (Al-Cu-Mg-Mn) Al-alloy with 25% vol. with SiC particles were used. All of the materials were produced by Aerospace Metal Composites (U.K.), which were referred to as AMC 225 (25% vol. 2-3 μ m SiC_p). The materials were extruded as a circular bar with two meters long. Prior to the machining process a solution treatment was applied which was at 505 C for 1hour, followed by cold water quenching after that nat-

ural ageing (T4) at room temperature for 100hour. Cyclic fatigue tests on MMCs were carried out on a computer controlled Instron servo-hydraulic test system. Load controlled fatigue tests employed at 1 Hz sine waveform, with the effect of mean stress assessed using R ratio (R=0). The alloy composition is given in Table 1. A laboratory fatigue specimens were machined using polycrystalline diamond. All tests were performed twice and their average values were taken. The parallel sided, double edge notch (DEN) specimens with its 3mm radius notch and average elastic stress concentration factor $K_t = 1.9$, semi circular Round Edge Notch (RCN) specimens with $K_t = 1.4$, and "V" Circular Notch (VCN) specimens with $K_t = 2.7$, have been employed. Some LCF fatigue data were used for the predictions. Detailed information and experimental results about LCF were given in Reference 3 and 5. The geometries and dimensions of the specimens were shown in Fig. 1. The fracture surfaces of specimens were examined in a scanning electron microscope to determine the predominant fracture modes and to characterise the fine scale topography of the fatigue fracture surfaces, JEOL 35 c SEM, was used.

TABLE 1

Chemical composition of the composites

Element	Cu	Mg	Mn	Fe	Zn	Si	Cr	Others	Al
Weight %	4-4.4	1.3-1.6	0.5	0.3 max	0.25	0.2	0.1	0.45 total	Balance

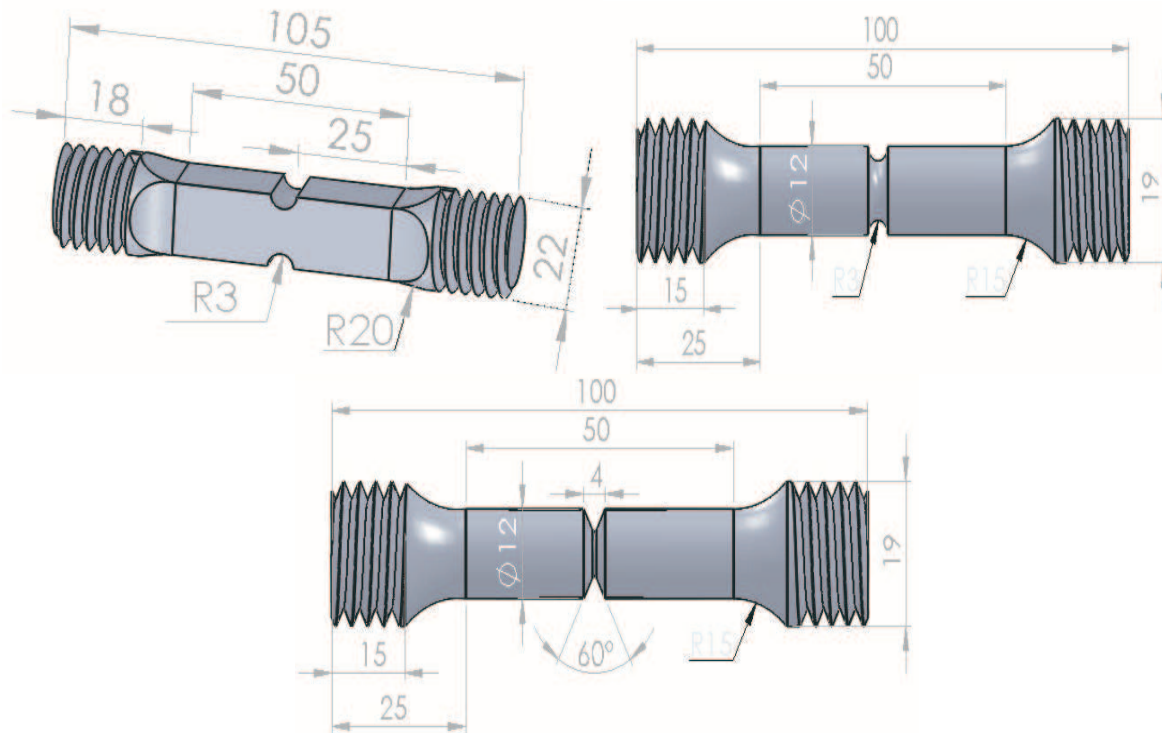


Fig. 1. The geometries and dimensions of the a) DEN, b) RCN, c) VCN specimens

3. Results and discussions

3.1. Notch severity effects

S-N data for three different notch geometries were presented in Figure 2. The graphs show how the fatigue life of AMC 225 composite material decreased with increasing stress concentration factor (K_t). The K_t factors are 2.7 (VCN), 1.9 (DEN), and 1.4 (RCN). Best fit curves were constructed by exponential equation that was shown in the same figure. The curves suggest that the least severe notched specimen (RCN) was the most resistant to crack initiation, while the sharpest notch (VCN) was the least resistant. Similar effects of notch severity on fatigue performance have been reported for 1045 steel

under constant amplitude, R=-1 loading. The effects are especially pronounced in the HCF region [7]. The peak elastic stress (σ_{actual}) at the notch root can be obtained by multiplying the stress concentration factor by applied maximum stress:

$$\sigma_{actual} = K_t \cdot \sigma_{nominal} \tag{1}$$

When data were re-expressed as (peak elastic stress) $K_t \sigma_{nom}$ against number of cycles, the DEN and RCN data superimposed, but the VCN gave more cycles for a given peak elastic stress (see Figure 3). This can be related with the increased concentration at the root of notch associated with a different stress state.

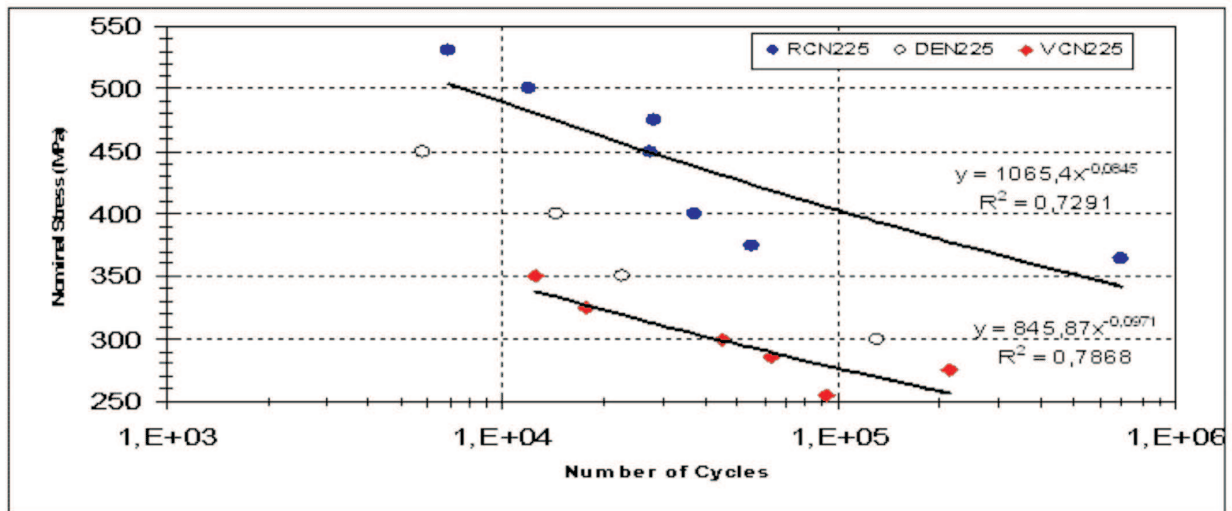


Fig. 2. Three different notch geometries effects on the fatigue life response of AMC 225 composite material tested in laboratory air at R=0

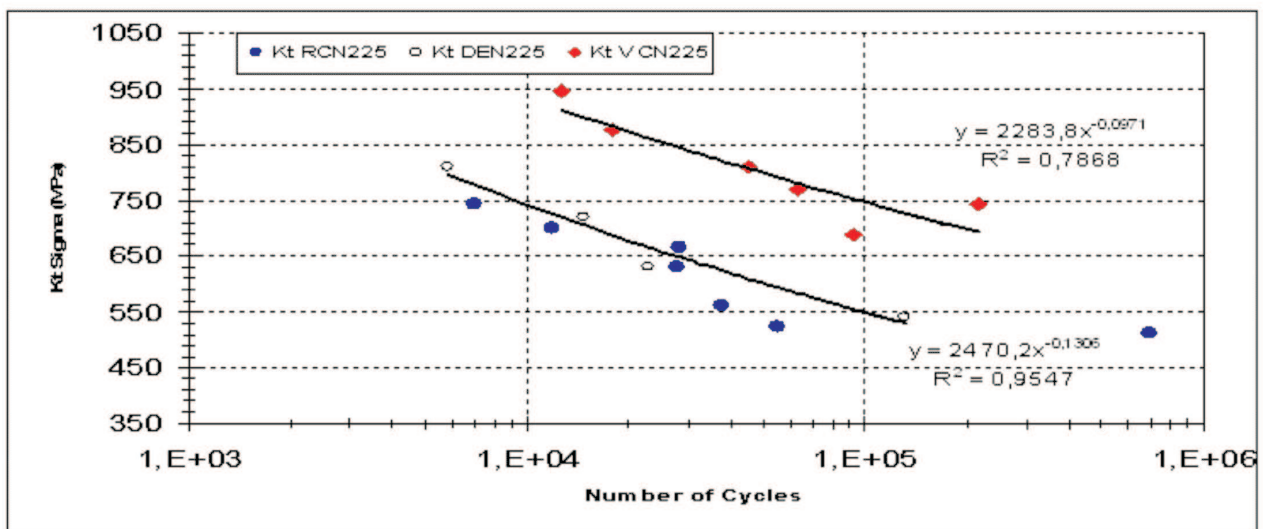


Fig. 3. Peak elastic stress against number of cycles to failure for AMC 225

3.2. Fatigue life predictions

Life predictions based on either stress life or strain life curves were widely reported for monolithic materials [8]. The critical strain life prediction method was applied to the notch test pieces in this study. The constants and coefficients used in the calculations were given in Table 2. Those constant and the monotonic tensile test parameters (E , σ_y , UTS) were used to predict fatigue life for three individual notch geometries. The calculation of the fatigue life for each notch geometry was based on the Coffin-Manson equation:

$$\Delta\varepsilon_t = C_p(N_f)^{\alpha_1} + C_e(N_f)^{\alpha_2} \quad (2)$$

Where $\Delta\varepsilon_t$, the total strain range, N_f , the number of cycles, α_1 , plastic strain exponent, α_2 , elastic strain exponent, C_p , plastic strain constant, and C_e , elastic strain constant at $N_f = 1$. Details about LCF of these composites were discussed in reference [3]. The critical strain technique assumes that if a plain specimen and a notch are loaded under identical strain conditions, they will fail in the same number of cycles. To apply this approach, the strain and stress at the critical notch must be determined. Estimation of the notch tip stress-strain of the material, Neuber's rule or Glinka's methods were used in general [9]. In this study, stress and strain values were obtained using the Neuber relationship. The Neuber's rule [10] states that the theoretical stress concentration, K_t , is equal to the geometric mean of actual stress and strain concentration:

$$K_t = \sqrt{k\sigma \cdot k\varepsilon} \quad (3)$$

Where $k\sigma$ = actual stress concentration = $\Delta\sigma/\Delta\sigma_n$, $k\varepsilon$ = actual strain concentration $\Delta\varepsilon/\Delta\varepsilon_e$, on submission Equation (3) becomes:

$$K_t = \sqrt{(\Delta\sigma/\Delta\sigma_n) \cdot (\Delta\varepsilon/\Delta\varepsilon_e)} \quad (4)$$

If the nominal stress and nominal strain are elastic, then the Equation (4) becomes:

$$K_t \cdot \Delta\sigma_n = (\Delta\sigma \cdot \Delta\varepsilon \cdot E)^{1/2} \quad (5)$$

With K_t is the theoretical stress concentration factor and E is the Young Modulus.

TABLE 2
Coefficients to describe the strain control fatigue response of MMCs

R ratio	Material	α_1	C_p	α_2	C_e
0	AMC225	-0.311	0.0553	-0.0088	0.00223
0.5	AMC225	-0.193	0.02511	-0.00876	0.0063
-1	AMC225	-0.139	0.0199	-0.00876	0.00112

According to the Neuber relationship, stress distribution takes place from the peak elastic stress $K_t\Delta\sigma_n$,

to the cyclic stress strain curve, according to the relationship $\sigma \times \varepsilon = \text{constant}$. The point of intersection of this hyperbole with the stress-strain curve determines the maximum stress and strain at the root of specimen. Applying the same technique to the unloading half-cycle allows the local strain range to be defined. The Neuber stress-strain distribution of each notch geometry was given respectively in Figure 4. a-c. The maximum stress and strain at the notch root was given by the point of intersections of the cyclic stress-strain curve. These values were used in the calculation of fatigue lives for each particular case. The predicted fatigue lives for the notch geometries were shown in Figure 5.a-c. The data were presented as a net section stress against cycles to failure. It can be seen that very good predictions can be obtained by critical strain approach, but when they include mean stress on these data, the fatigue lives become lower, so just critical strain prediction was applied for the rest of data. A good correlation was demonstrated for the DEN and VCN notch geometry however some of the HCF data was lower than predicted values for the RCN. Although the prediction of fatigue life can be conservative as stress levels approach in the fatigue endurance regime, the predictions in all cases within the LCF regime (cycles $\leq 50,000$) were considered to be very favorable. This question is a common problem of the fatigue life models, it is hard for one model to cover both HCF and LCF ranges very well. Similar to our results, the predictions with the modified equivalent strain range method, gave accurate correlation with the LCF experimental results, but it was not in the HCF region [11]. Also, recently linear and bi-linear stress-life models were applied to predict HCF region of various Al alloys [12]. For severe notches (VCN) fully reversed plasticity would occur, for this reason, strain control data generated under $R=-1$ conditions were used to predict the notch behavior. Same method was also applied to predict for the 17% vol. SiC_p composites [13]. Also an alternative method was used to assess notch data is; to consider $K_t\Delta\sigma$ the peak elastic stress range which adds to the stabilized stress range included at the stabilized condition during strain control tests. This method recognizes the fact that, the stress range plays a significant role in the initiation of fatigue cracks. Moreover, an analytical model for predicting the crack initiation life of LCF of discontinuously reinforced MMCs has been proposed on the basis of Gibbs free energy law. In this model, the formation of a fatigue crack was considered to be associated with the reduction of the internal energy that could be expressed as a part of the area of saturated hysteresis loop [14].

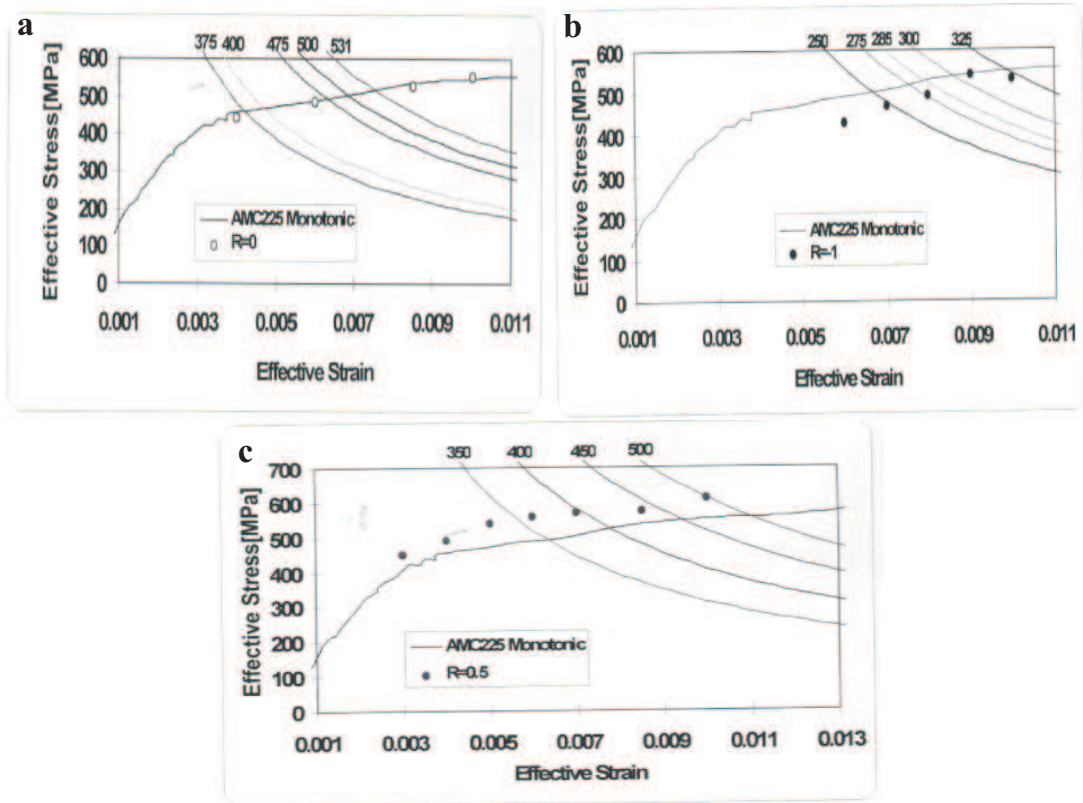


Fig. 4. Neuber stress-strain distribution for AMC225 with a) DEN b) VCN and c) RCN specimens

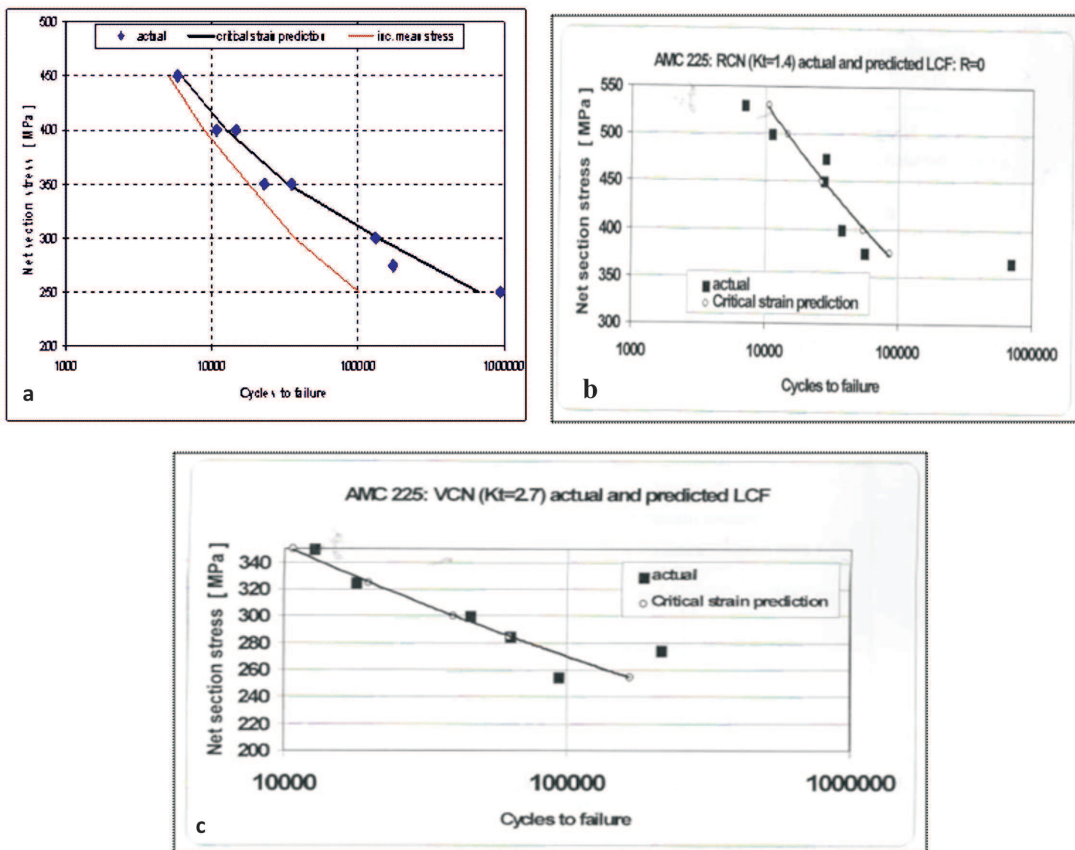


Fig. 5. a. Fatigue life prediction DEN notches at R=0.5 for AMC 225 with critical strain and including mean stress conditions. b) RCN at R=0 and, c) VCN at R=-1

3.3. Crack path particle interactions

A large number of test pieces encompassing the full range of size and volume fraction of SiC_p were examined. However, only AMC 225 is considered here. Typical fatigue crack initiation of VCN specimen was shown in Figure 6.a where there are two crack initiation sites. Multiple surface crack initiation sites were considered to be common in 2xxx series Al-alloy MMCs and generally associated with SiC_p clustering, large SiC_p (bigger than average particle size), or intermetallic particles (Fe, Si, Cu, Mg rich) [7,15,16]. Also, triaxial stress and straining were pronounced more for the VCN sample, thus it may be the reason for the multiple crack sites. Apparently, crack initiation event occurred at the 'weakest' macro and microstructural locations. The local stress and strains developed in the 'weakest' microstructural locations, where voids and microcracks formed. Nucleation of voids and the formation of small microcracks at the particles appeared to control the tensile strength and ductility of the composites [17].

Typical crack path particle interactions can be seen in Figure 7a and b. The crack path was considerably flat and smooth in this material. Also in Fig. 7 a. demonstrates how to the SiC_p and intermetallic small particles were preferably aligned, parallel to the extrusion direction which is perpendicular to the crack growth direction in the test specimen. The dispersion of ceramic particles in the metallic alloys induces a number of microstructural changes in the metallic matrix (enhanced dislocation density, smaller grain size, weaker texture etc.) which promote homogenous slip and inhibit the formation of slip bands [18].

Although, crack propagation in the reinforced alloy occurred predominantly in the matrix material, SiC_p played a significant role in the influencing of the crack path. There was a significant crack deflection caused by relatively large reinforcement particles and surface deco-

hesion obtained by fine particles (Fig.7a and b). The fine SiC_p did not crack easily, but they were responsible for a large strain difference between the plastically deforming ductile matrix and elastically deforming hard and brittle reinforcement. This difference can lead to decohesion of the particle matrix interfaces. The fracture stress of brittle SiC_p has been expressed in terms of equation [19-20]:

$$\sigma_{\text{SiC}} = [\pi \cdot E \cdot G_{pm} / 2(1 - \nu^2) P_z]^{1/2} \quad (6)$$

where, E , elastic modulus, ν , the Poisson's ratio, G_{pm} , the critical strain energy release rate and P_z , the particle size. According to the above relationship, the fracture stress is inversely related to the P_z of the reinforcement. For a constant volume fraction of reinforcement, the tendency for SiC_p to fracture is greatest when the P_z is high (see Fig.6b). Composite materials with coarse particles exhibit a higher number of cracked particles at a given stress or strain level, compared to those with fine particles, because of the high fracture stress of the latter [5]. Thus, the calculated fracture stress of $5\mu\text{m}$ SiC_p was 780MPa but for $1\mu\text{m}$ SiC_p was 1744MPa in 2xxx series Al-alloy composites [21]. High magnification SEM studies showed that the crack appeared to seek out regions where they had clustered or coarse SiC_p . This process was enhanced because of the local stress state near the crack tip of the reinforcement which was much higher than the average stress. The local stress concentration causes constrained plastic flow which leads to voids initiating and growing along the interfaces between the reinforcement and Al-alloy matrix. The voids link up and allow the main crack to progress to the next high stress region where the crack is arrested until further voids form. Consequently, it is not surprising to find that the crack path and growth rates are irregular with the crack frequently jumping between areas with a dense population of SiC_p but slowing in regions where the matrix dominates.

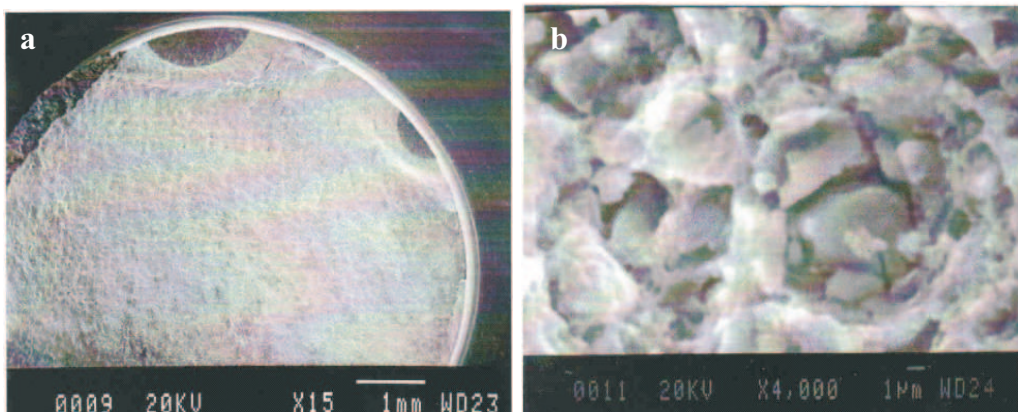


Fig. 6. a. Multiple crack initiation sites b) particle cracking in the large reinforcement

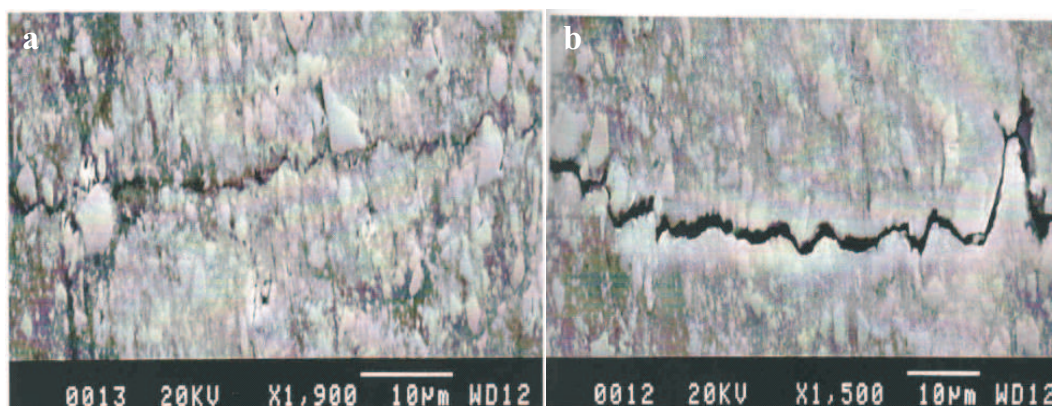


Fig. 7. SEM pictures of AMC 225 a) Distribution of fine particles through the extrusion direction and crack path seeking relatively large particles b) decohesion between matrix-particle interfaces and crack path deflection in the matrix

4. Conclusions

In this study, fatigue responses of 2124 Al-SiC_p MMCs were investigated with three different notch geometries. The S-N curves of this composite were shifted down due to the severity of notches. Also, critical strain approach was used to predict to fatigue life of materials. Method can be easily used for the LCF region, but it underestimates the life of the material in HCF region. Hence, energy related or crack propagation related fatigue life estimations can be adopted in this model to predict better fatigue life, particularly in the HCF region. Also, the finite element method can be used to predict the stress-strain response of the notches. Most of crack initiation sites related with the microstructural defects, like large reinforcement particles or intermetallic particles. The distribution of fine and coarse particles inside the matrix materials significantly affected the crack path. Uniform distribution of these particles was crucial for the determination of the materials toughness and ductility. Thus, agglomerations of fine particles and more than average particles may be avoided.

Acknowledgements

The Author thanks Prof. Dr. W.J. Evans and Prof. Dr. M.R. Bache at the University of Wales, SWANSEA for their great assistance and support. The work described here was carried out in the department of Materials Engineering at University of Wales, Swansea.

REFERENCES

- [1] I. Uygur, Iranian J. Sci. Technol, 28B2, 239 (2004).
- [2] I. Uygur, W.J. Evans, M. Bache, B. Gulenc, Metallo. Novei. Tekhnol, 26, 927 (2004).
- [3] I. Uygur, and M.K. Kulekci, Turk. J. Eng. Env. Sci. 26, 265 (2002).
- [4] J. Schijve, Int. J. Fatigue 25, 679 (2003).
- [5] I. Uygur, PhD Thesis (Swansea: University of Wales:1999).
- [6] F. Ellyin, Fatigue damage, crack growth and life prediction. London, Chapman & Hall, 1997.
- [7] C. MacDougall, and T.H. Topper, Int. J. Fatigue 19, 389 (1997).
- [8] T.H. Topper, and T.S. Lam, Int. J. Fatigue 19, 137 (1997).
- [9] J.Y. Lim, S.G. Hong, S.B. Lee, Int. J. Fatigue 27, 1653 (2005).
- [10] H. Neuber, J. Appl. Mech. Trans. ASME, E28, 544 (1961).
- [11] B. Li, L. Reis, M. Freitas, Int. J. Fatigue 28, 451 (2006).
- [12] A. Fatemi, A. Plaseied, A.K. Khosrovaneh, D. Tanner, Int. J. Fatigue 27, 1040 (2005).
- [13] M.R. Bache, W.J. Evans, I. Uygur, Mater. Sci. & Tech. 14, 1065 (1998).
- [14] Q. Zhang, D.L. Chen, Int. J. Fatigue 27, 417 (2005).
- [15] N.J. Hall, J.W. Jones, A.K. Sachdev, Mater. Sci. & Eng. A83, 69 (1994).
- [16] J.J. Bonnen, J.E. Allison, J.W. Jones, Metall. Trans. 22A, 1007 (1991).
- [17] W.M. Zang, G.L. Esperance, M. Suery, Mater. Sci. & Eng. A214, 104 (1996).
- [18] J. Llorca, Prog. Mater. Sci. 47, 283 (2002).
- [19] T.S. Srivatsan, and R. Auradkar, Int. J. Fatigue 14, 355 (1992).
- [20] T.S. Srivatsan, R. Auradkar, and A. Parash, Eng. Frac. Mech. 40, 295 (1991).
- [21] B. Wang, C.M. Janowski, and B.R. Peterson, Metall. Trans. 26A, 2457 (1995).